Research Square

Preprints are preliminary reports that have not undergone peer review.
They should not be considered conclusive, used to inform clinical practice,
or referenced by the media as validated information.

Estimation of Daily Reference Evapotranspiration using Machine Learning and Deep Learning Techniques with Sparse Meteorological Data

Ajit Kumar Nayak

Ajit.Nayak@icar.gov.in

ICAR-Indian Institute of Water Management

A Sarangi

ICAR-Indian Institute of Water Management

S Pradhan

ICAR-Indian Institute of Water Management

R K Panda

ICAR-Indian Institute of Water Management

N M Jeepsa

ICAR-Indian Institute of Water Management

B S Satpathy

ICAR-Indian Institute of Water Management

Mithlesh Kumar

Odisha University of Agriculture and Technology

Research Article

Keywords: Evapotranspiration, machine learning, deep learning, support vector regression, XGBoost, KNN regression, random forest, LSTM

Posted Date: September 3rd, 2024

DOI: https://doi.org/10.21203/rs.3.rs-4853172/v1

License: This work is licensed under a Creative Commons Attribution 4.0 International License.
Read Full License

Additional Declarations: No competing interests reported.

Estimation of Daily Reference Evapotranspiration using Machine Learning and Deep Learning Techniques with Sparse Meteorological Data

Ajit Kumar Nayak[1*], A Sarangi[1], S Pradhan[1], R K Panda[1], N M Jeepsa[1], B S Satpathy[1], Mithlesh Kumar[2]

[1]*ICAR-Indian Institute of Water Management, Bhubaneswar, 751023, Odisha, India*

[2]*College of Agricultural Engineering and Technology, Odisha University of Agriculture and Technology, Bhubaneswar, 751003, Odisha, India*

*Corresponding author's E-mail: Ajit.Nayak@icar.gov.in / anayak62@gmail.com

Abstract

Accurate estimation of evapotranspiration is very crucial for enhancing the real time irrigation scheduling and decision making in water resources planning. Traditionally, empirical methods are used to calculate the reference evapotranspiration using available meteorological data. However, in many areas, such data is limited or unavailable for ET_o estimation. Hence, this study aims to explore data-driven models like machine learning (ML) and deep learning (DL) for estimating ET_o with minimal meteorological data. In this study, five ML models, including linear regression (LR), random forest (RF), support vector regression (SVR), XGBoost, KNN regression, and two deep learning methods such as feedforward neural networks and long-term short-term memory (LSTM), were used to estimate the reference evapotranspiration (ET_o) over the Phulnahara canal command area using various combinations of meteorological parameters. The results of these models were compared with the Penman-Monteith-based ET_o. The Penman-Monteith-based ET_o exhibits a significant positive correlation with sunshine hour and maximum temperature, displaying correlation coefficients of 0.8 and 0.6, respectively, while RHmin and RHmax demonstrate a negative correlation. The findings revealed that when all climate data is available, the coefficient of determination (R^2) rises to 0.98. However, when data is limited, it drops to 0.78. The SVR model outperformed other ML models with all input combinations. However, KNN emerged as the most reliable model for estimating ET_o with input data of maximum and minimum temperature. Interestingly, we found that even using just three parameters (temperature, wind speed, and relative humidity) or two-parameter combinations (temperature and relative humidity or temperature and wind speed) can yield promising results in ET_o estimation. The findings of this study offer valuable insights for estimating ET_o in regions with limited climate data, which is crucial for effective agricultural water management.

Keywords: Evapotranspiration, machine learning, deep learning, support vector regression, XGBoost, KNN regression, random forest, LSTM.

1. Introduction

Evapotranspiration (ET) is an important factor in defining regional water balance since it takes into account the interaction of soil, vegetation, and atmosphere (Bijlwan et al., 2024). Research shows that an astounding 90% of the water used in agriculture is lost as a result of crop evapotranspiration (Rana and Katerji, 2000). Quantifying evapotranspiration enables the reduction of water waste, improvement of irrigation efficiency, facilitation of effective irrigation, and enhancement of water use efficiency (Sattari et al., 2021). Therefore, accurately estimating evapotranspiration (ET) is essential for comprehending hydrological and natural processes, reducing agricultural drought, effectively managing water resources, and ensuring efficient operation and control of irrigation schedules (Chia et al., 2020; Amani and Shafizadeh-Moghadham, 2023; Yong et al., 2023; Bijlwan et al., 2024; Chia et al., 2022). Due to its significance, numerous researchers have dedicated much time and effort to find strategies for overcoming the challenges associated with estimating it, particularly in situations where there is a lack of sufficient meteorological data (Yong et al., 2023; Treder et al., 2023).

Typically, the equations used to compute evapotranspiration are intricate, non-linear, incorporate randomness, and are based on certain underlying assumptions (Sattari et al., 2021). Researchers have presented numerous methods to compute evapotranspiration (ET), dividing them into two groups: direct and indirect approaches (Amani and Shafizadeh-Moghadham, 2023). The direct approach includes lysimeter, water budget measurements, eddy covariance, Bowen ratio, scintillometry, sap flow, etc. (Huang et al., 2019; Ayaz et al., 2021; Bijlwan et al., 2024). According to Irmak et al. (2003) and Tikhamarine et al. (2019), these direct methods are costly, laborious, time consuming, inconvenient, and subject to spatial and temporal constraints. Indirect techniques are experimental and quasi-experimental based equations, which have been designed to estimate the ET while taking into consideration the elements that affect it (Amani and Shafizadeh-Moghadham, 2023). According to the Food and Agriculture Organisation (FAO), the Penman-Monteith method, which is the most popular method to estimate the ET, requires a comprehensive set of climatic data such as relative humidity, air temperature, solar radiation, and wind speed (Aly et al., 2024). Establishing and maintaining weather stations to gather these data is difficult, particularly in underdeveloped nations where wind speed and sun radiation data are rarely available (Treder et al., 2023). Hence, it is imperative to develop alternative methods that rely on a limited amount of meteorological data while maintaining a high level of accuracy.

In recent decades, machine learning techniues have emerged as viable alternatives to direct and indirect methods. They have gained significant popularity for estimating evapotranspiration in

various geographical climatic locations worldwide. The utilisation of data-driven models to predict evapotranspiration has witnessed a surge in recent years, mostly attributed to the need to unravel its intricate linkages with the predictors, especially for nonlinear and multi-variable functions (Fan et al., 2018; Bellido-Jiménez et al., 2021). Machine learning algorithms utilize extensive datasets and powerful computer tools to accurately predict ET by identifying complex relationships and trends in the data. Furthermore, satellite imagery, historical weather data, and ground-based evapotranspiration observations are used to train these models (Bijlwan et al., 2024; Shiri et al., 2014).

In recent years, many researchers have focused on machine learning methods to predict reference evapotranspiration (ET_o) for different crop types in various geographical places around the world. Tikhamarine et al. (2019) estimated the monthly reference evapotranspiration (ETo) at two stations, Dar El Beida (Algeria) and Ranichauri (India), using five hybrid machine learning models: artificial neural network (ANN)-embedded grey wolf optimizer (ANN-GWO), particle swarm optimizer (ANN-PSO), whale optimization algorithm (ANN-WOA), multiverse optimizer (ANN-MVO), and ant lion optimizer (ANN-ALO). The results revealed that ANN-GWO outperformed the others. Sammen et al. (2023) employed four regression-based machine learning approaches, namely support vector machine (SVM), Bagged trees algorithm (BaT), random forest (RF), and Boosting trees algorithm (BoT), to simulate daily reference evapotranspiration in semi-arid region of Iran. The results revealed that the random forest (RF) method achieved the highest accuracy, followed by the BaT, BoT, and SVM methods. Yong et al. (2023) tested the performance of three standalone machine learning (ML) models, the light gradient boosting machine (LGBM), artificial neural network (ANN), and decision forest regression (DFR), using four different combinations of climatic variables in East Coast Economic Region of Malaysia. The results showed that the LGBM and ANN models performed well overall and were recommended as alternatives for ET estimate. Similarly, Ayaz et al. (2021) compared four machine learning models: Long short-term memory neural networks (LSTM), Gradient Boosting Regressor (GBR), Random Forest (RF), and Support Vector Regression (SVR) to assess their ability to estimate evapotranspiration with minimal climatic input variables in two different climatic regions: Waipara (New Zealand) and Hyderabad (India). The results revealed that the LSTM model outperformed other machine learning models across all input combinations at both stations.

Treder et al. (2023) investigated the performance of four machine learning techniques (regression trees, random forests, boosted trees, and artificial neural networks) in estimating evapotranspiration using limited weather data. The results showed that the employed models could capture nonlinear interactions between meteorological variables and evapotranspiration. Furthermore, the accuracy of evapotranspiration estimation was determined by the type of input data and the machine learning model utilized, with the ANN model producing the best

evapotranspiration prediction results. Bijlwan et al. (2024) used artificial neural networks (ANN), LGBM regressors, and gradient boosting regressors (GBR) to estimate reference evapotranspiration using historical weather data from the experimental plots at Govind Ballabh Pant University of Agriculture and Technology in Pantnagar, Uttarakhand state, India. The data demonstrated that LGBM outperformed the others. In order to model the monthly mean daily ET_o using maximum and minimum air temperatures as well as extraterrestrial solar radiation data from 15 stations located in the Jiangxi Province of China, Wu et al. (2019) assessed the performance of eight machine learning models: Artificial Neuron Network (ANN), Extreme Gradient Boosting (XGBoost), Random Forest (RF), Gradient Boosting Decision Tree (GBDT), Support Vector Machine (SVM), Extreme Learning Machine, Multivariate Adaptive Regression Spline (MARS), and a novel Kernel-based Nonlinear Extension of Arps Decline (KNEA) Model. The empirical Hergreaves-Samani (HS) model was used to compare the results of these machine learning models. The findings demonstrated that, in local applications, the tree-based models (RF, GBDT, and XGBoost) had better prediction accuracy than the other models. The MARS and SVM models outperformed the others when temperature data was the sole available information, whereas the ANN and HS models underperformed.

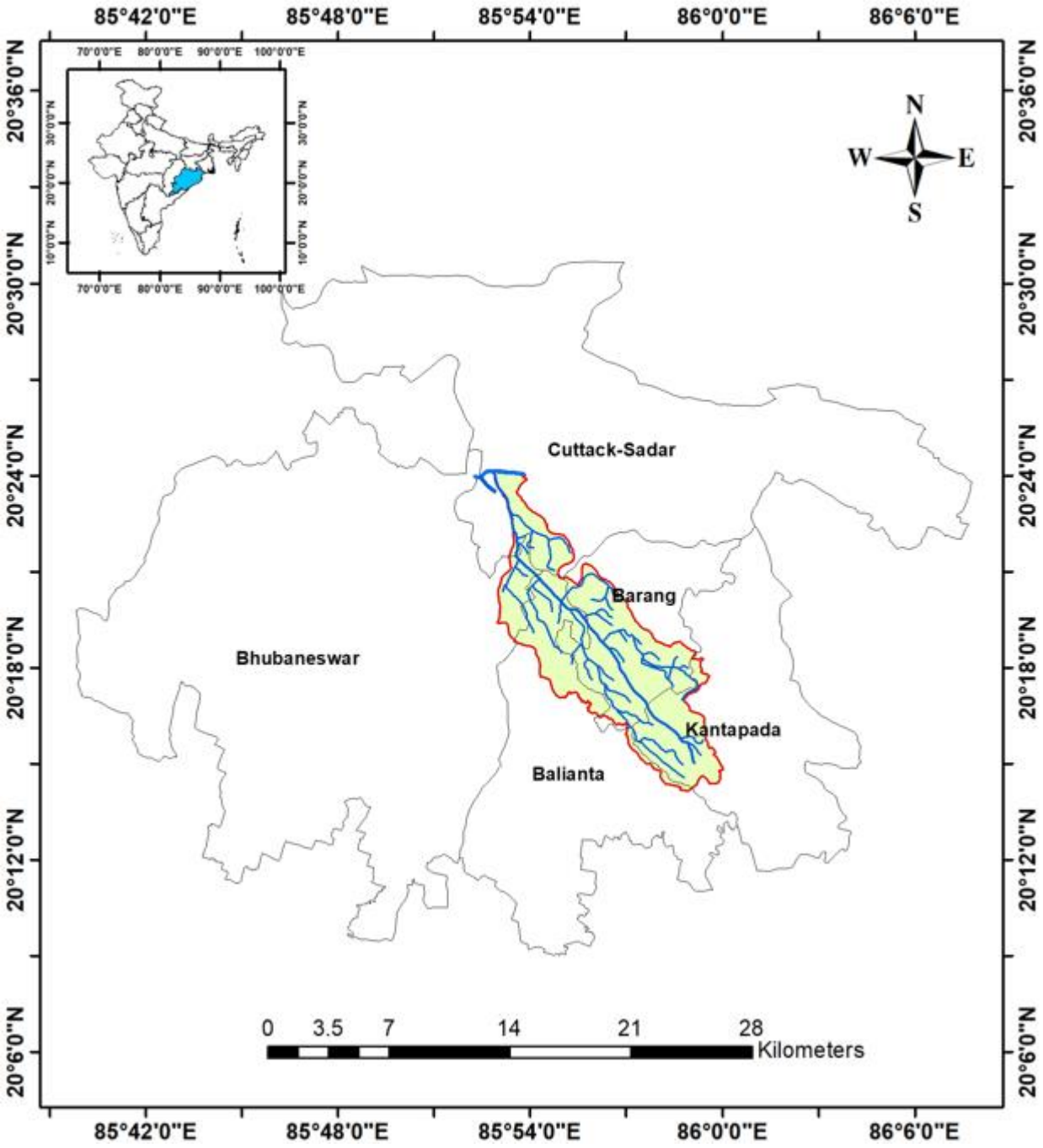
The present study uses novel techniques to precisely estimate the daily reference evapotranspiration (ET_o) in the Phulnakhara canal command region of Odisha, India. The research encompasses a wide array of models, including both machine learning and deep learning models. In order to address the issue of restricted availability of metrological data, the study examines four different scenarios: firstly, utilizing all six parameters of Penman-Monteith as input; secondly, excluding sunshine hour while incorporating all other weather variables; thirdly, integrating temperature and relative humidity; and lastly, taking only temperature as input variables. We conduct a detailed comparison of these models to determine the best model for reference evapotranspiration (ET_o) estimation under various data availability conditions, with the goal of improving prediction accuracy.

2. Materials and Methods

2.1 Study area

The Phulnakhara distributary canal command area, which is part of the Puri main canal system, is located approximately 28 meters above mean sea level and extends between 20°19'15" N to 20°14'56" N latitude and 85°52'51" E to 86°95'96" E longitude (Fig. 1). The Phulnakhara distributary, which runs for 21.410 km, takes water from the Kakatpur branch canal of the Puri main canal system. The command area comprises 7 minors and 33 sub-minors. The cultivable command area of the distributary is approximately 4903.29 ha, with a design discharge of 6.03

cumec. Paddy and maize are the major *kharif* crops, and green gram, blackgram, and groundnut are the dominant *rabi* crops.



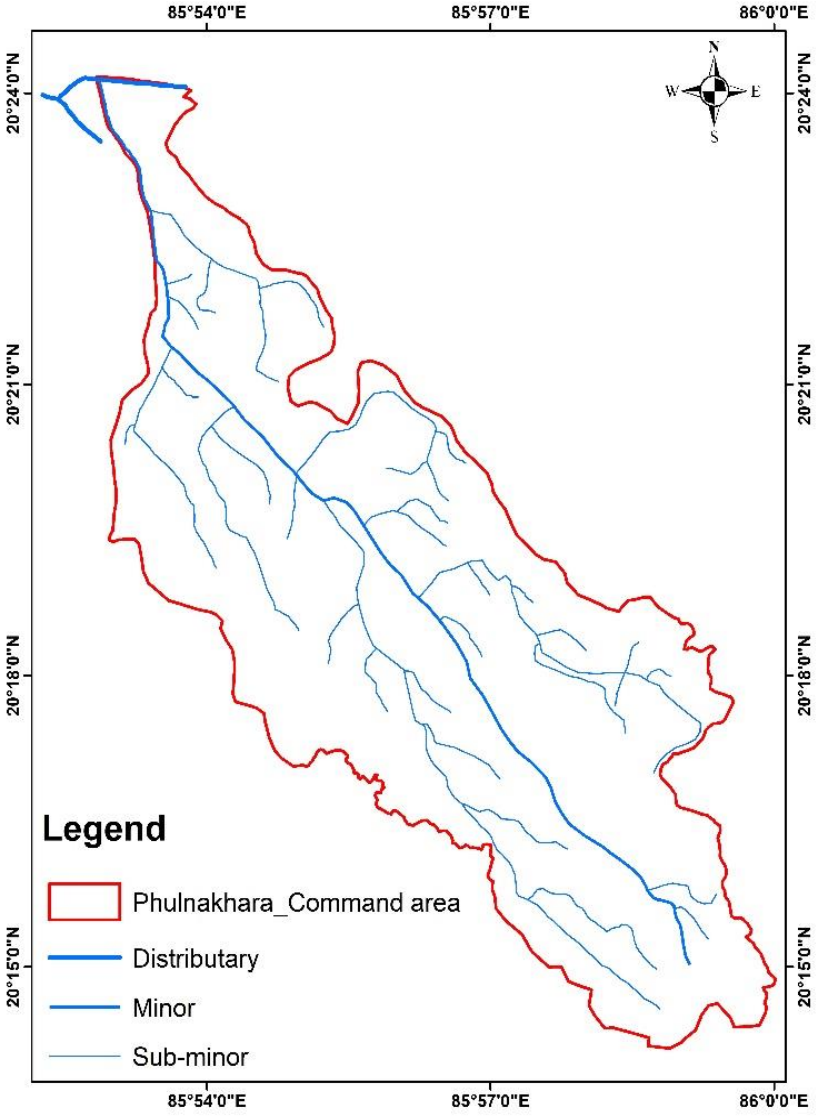


Fig. 1. Location of the Phulnakhara canal command area

2.2 Data collection

All the metrological data from 1961 to 2020 was collected from the ICAR-NRRI, Cuttack, and the statistical details of the input data for the study are shown in Table 1. In this study, 80% of the total dataset was used for model training and 20% for testing. Figure 2 displays the flow chart that explains the details of various models.

171 **Table 1: Descriptive statistics of daily meteorological data**

172

Parameters	Tmax (°C)	Tmin (°C)	RHmax (%)	RHmin (%)	Sunshine (hours)	Wind speed (kmph)	ET_o (mm)
Maximum	46.10	36.20	100.00	100.00	12.00	201.00	10.46
Minimum	23.32	12.30	45.34	20.26	0.00	7.06	1.14
Mean	31.85	22.25	90.61	57.90	6.57	5.02	4.28
Standard deviation	3.65	4.70	6.26	18.29	3.34	3.86	1.42

173

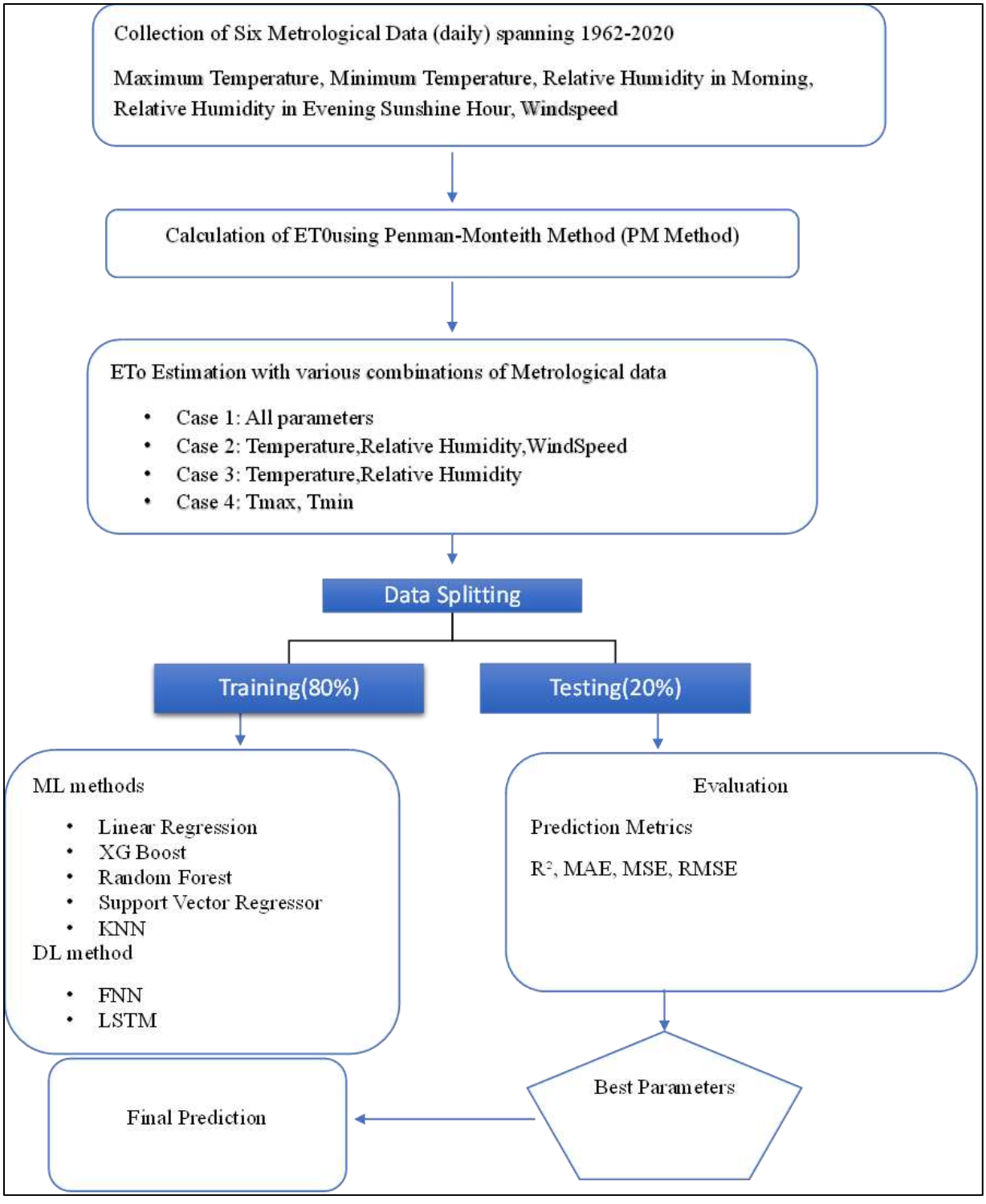


Fig. 2. Flow chart of the methodology for the ET_o estimation

3. Methodology

The ET_o values calculated using the Penman-Monteith method are used as ground truth benchmarks for training and testing various machine learning and deep learning models.

3.1 FAO Penman-Monteith method

In this paper, we utilized the Penman-Monteith method to calculate the mean daily ET_o from daily meteorological data, which served as the reference data for testing machine learning and deep learning models (Kumar et al., 2002; Song et al., 2019).

$$ET_o = \frac{0.408\Delta(Rn-G)+\gamma u_2 \frac{900}{T+273}(e_s - e_a)}{\Delta+\gamma(1+0.34u_2)} \quad (1)$$

Where, ET_o = reference evapotranspiration (mm/day), Δ= slope vapor pressure curve (k pa°/C), Rn = net radiation (MJ/m^{2}d), G = soil heat flux (MJ/m^2 d), u_2 = wind speed measured at 2 m height (m/s), $(es - ea)$= vapor pressure deficit in the air at 2 m height (k Pa), T = mean temperature at 2 m height daily basis (°C), γ = psychrometric constant (k pa°/C).

3.2 Machine learning models

In this study, five machine learning (ML) models, namely linear regression, k-nearest neighbors (KNN) regression, random forest (RF), support vector regression (SVR), and XG Boost, and two deep learning (DL) models, namely feed forward neural network and Long Short-Term Memory (LSTM), were employed to estimate the ET_o over the Phulnakhara distributory command area. The comparative performance was conducted by dividing the whole dataset into training and testing periods. In this study, 80% of the total datasets were used for training the ML and DL models, and the remaining 20% were employed for testing and validation purposes.

3.2.1 Linear regression

In the realm of regression models, the independent variables serve as predictors for the dependent variables. Essentially, regression analysis seeks to estimate the value of the dependent variable ‘y’ based on a spectrum of values within the independent variable ‘x’ (Schmidt & Finan, 2018). It is important to note that regression approaches can manifest in either simple linear regression or multiple regression (Maulud & Abdulazeez, 2020; Song et al., 2019).

(i) Simple linear regression

Simple linear regression is a fundamental model that operates with just one independent variable. This model serves as a valuable tool for dissecting the impact of independent variables, allowing us to discern their influence apart from any potential interplay with dependent variables (Huang, 2022). Essentially, we express the simple linear regression equation as follows:

$$y = \beta_0 + \beta_1 x \, . \tag{2}$$

(ii) Multivariate linear regression

Multivariate linear regression (MLR) is a statistical method that considers multiple explanatory variables to forecast the outcome of a response variable (Shiri et al., 2014). The primary objective of MLR is to establish a linear model that captures the relationship between the independent variables (denoted as 'x') and the dependent variable (denoted as 'y') for subsequent analysis (Mallikarjuna et al., 2012). The fundamental MLR model as follows:

$$y = \beta_0 + \beta_1 x_1 + \cdots + \beta_m x_m + \varepsilon \tag{3}$$

In this equation, y represents the dependent variable, while x_1, x_2,..., x_m are the independent variables (Dimitriadou & Nikolakopoulos, 2022). The coefficients β_0, β_1,..., β_m are the parameters to be estimated, and ε represents the error term. The MLR model aims to determine the best-fitting linear relationship between these variables, allowing us to make predictions and gain insights into the underlying relationships within the data. The formula to determine the matrix is as follows:

$$\hat{\beta} = (X^T X)^{-1} X^T y \tag{4}$$

Where,

$$\beta = \begin{bmatrix} \beta 1 \\ \beta 2 \\ . \\ . \\ . \\ \beta m \end{bmatrix} X = \begin{bmatrix} 1 & x11 & x12 & . & . & . & x1m \\ 1 & x21 & x22 & . & . & . & x2m \\ 1 & x31 & x32 & . & . & . & x3m \\ . & \square & \square & \square & \square & \square & \square \\ . & \square & \square & \square & \square & \square & \square \\ 1 & xm1 & xm2 & . & . & . & xmm \end{bmatrix} Y = \begin{bmatrix} y1 \\ y2 \\ . \\ . \\ . \\ yn \end{bmatrix} \tag{5}$$

3.2.2 Random forest

Random forest (RF) is a versatile ensemble technique capable of handling both classification and regression tasks. It combines multiple tree predictions to determine the final output. In

252 classification, it uses majority voting, while in regression, it takes the average of the predictions
253 from individual trees. In supervised machine learning, the RF finds widespread application
254 (Biau, 2012; Biau & Scornet, 2016; Hao et al., 2022). The RF model can be expressed as
255 follows:
256
257 $$f(x) = f_1(x) + f_2(x) + f_3(x) + \cdots \quad (6)$$
258
259 Here, the overall model f is the sum of individual base models f_i, where each base model is a
260 simple decision tree.
261
262 The fundamental concept behind RF is to aggregate the predictions of multiple decision trees to
263 arrive at the final output, thereby the main idea behind RF is to combine the predictions of
264 several decision trees to get the final result. This lowers the risk of overfitting that comes with
265 each individual tree (da Silva Júnior et al., 2019). Random forests, also known as random
266 decision forests, effectively address the issue of overfitting that decision trees often face (Yin et
267 al., 2021). They achieve this by constructing a multitude of decision trees during training and
268 then aggregating the results. According to Breimanan (2001), in classification tasks, the final
269 prediction is based on the mode of classes, while in regression, it relies on the mean prediction
270 from the individual trees. However, a unique twist emerges during the decision-making process
271 at each node of the tree. Each tree receives a random subset of features instead of considering all
272 available features (Yin et al., 2021). Within this subset, the decision tree evaluates and selects the
273 best feature to split the data. This feature selection process often relies on mathematical criteria,
274 with the Gini Index being a common choice (Wang et al., 2019). Thus, the utilization of a
275 random feature subset at each node results in the generation of multiple decision trees that are
276 deliberately correlated for mitigating the risk of overfitting inherent in individual trees (Huang et
277 al., 2019).
278
279 **3.2.3 XGBoost**
280
281 The extreme gradient boosting, also known as the XGBoost algorithm, was introduced by Chen
282 and Guestrin (2016). The XGBoost stands as an implementation of gradient-boosted decision
283 trees, and it operates by generating decision trees sequentially. It is a versatile approach, serving
284 purposes in both the regression and classification problem domains. XGBoost is an ensemble
285 machine learning algorithm rooted in decision trees, employing a gradient boosting framework.
286 Further, the XGBoost algorithm has demonstrated its ability to lower computational costs while
287 delivering exceptional model performance (Chandrahas et al., 2022). The gradient boosted
288 decision trees are implemented by XGBoost, which generates decision trees in strict sequential
289 order. Within this algorithm, the utilization of weights assumes a pivotal role. We assign a weight
290 to each independent variable and then incorporate it into the decision tree to predict outcomes.

Notably, the tree increases the weights of variables it incorrectly predicts, and then feeds these adjusted variables into a subsequent decision tree. These individual classifiers or predictors collectively form an ensemble, resulting in a robust and highly accurate model (da Silva Júnior et al., 2019). XGBoost is renowned for its swift modelling process. It can construct complex ensembles of decision trees efficiently, making it an excellent choice for handling large datasets and real-time applications. When data is very large and does not fit into main memory, XGBoost divides it into multiple blocks and stores each block on the disk. The blocks are nicely compressed by the column and decompressed on the fly using an independent thread when they reach the disk, and this boosts the performance significantly (Mo et al., 2019).

3.2.4 Support vector regression

The support vector regression (SVR) has versatile applications in both classification and regression problems. It was initially introduced by Vapnik (1998). Boswell (2002) primarily employs the SVM as a machine learning technique, which operates by identifying a hyperplane capable of perfectly separating multi-dimensional data into distinct classes. The main goal of SVM modelling is to pick a hypothesis from a set of hypotheses that fits the target function as closely as possible while still leaving a certain amount of room for error (Gocić et al., 2015; Granata, 2019). The closest data points are called support vectors, and the space between these support vectors is referred to as the "margin." The ultimate objective of SVM is to establish an optimal separating hyperplane, which is the classifier that maximizes this margin. Within SVM, the primary objective revolves around fine-tuning the optimal separating hyperplane to maximize its capacity for generalization (Shiri et al., 2014). Even with a perfectly set hyperplane, the classifier may struggle to generalize well if the training data isn't separable in a straight line. Certain problems may demand a more flexible approach that allows for a broader range of potential outcomes. In these scenarios, we can adapt SVM to predict numerical values instead of discrete labels (Raza et al., 2020).

3.2.5 K-nearest neighbours (KNN)

Cover and Hart (1967) developed the k-nearest neighbor (KNN) technique, which is now frequently utilized in data mining models (Yamac, 2021). In KNN regression, we estimate the value of a dependent variable for a given data point by calculating the mean of the target values associated with its K closest neighbors within the training data. The value selection for K is a user-defined hyperparameter that dictates the quantity of nearest neighbors taken into account to formulate the prediction (Yamaç, 2021). Hence, KNN regression is categorized as an instance-based learning or non-parametric regression algorithm, relying on the training data to formulate predictions. Unlike traditional models, it doesn't create a specific model for making predictions on new data points (Wu et al., 2021). Instead, KNN makes predictions by considering

neighboring data points, and it operates without making any assumptions about the training dataset's underlying characteristics. The KNN regression doesn't base its predictions on such assumptions. Instead, it depends on discerning patterns within the data to make accurate predictions (Bayram & Çıtakoğlu, 2023). The KNN algorithm is a versatile regression method that can scale effectively, making it suitable for both extensive and limited datasets. Moreover, KNN regression, like its counterpart in KNN classification, can predict both continuous and categorical target variables (Yamaç & Todorovic, 2020). However, the pivotal aspect lies in selecting an appropriate value for K, as a small K value can lead to overfitting, while a large K value can result in underfitting, so an elbow curve was prepared and a K value of 9 was chosen (Fig. 3).

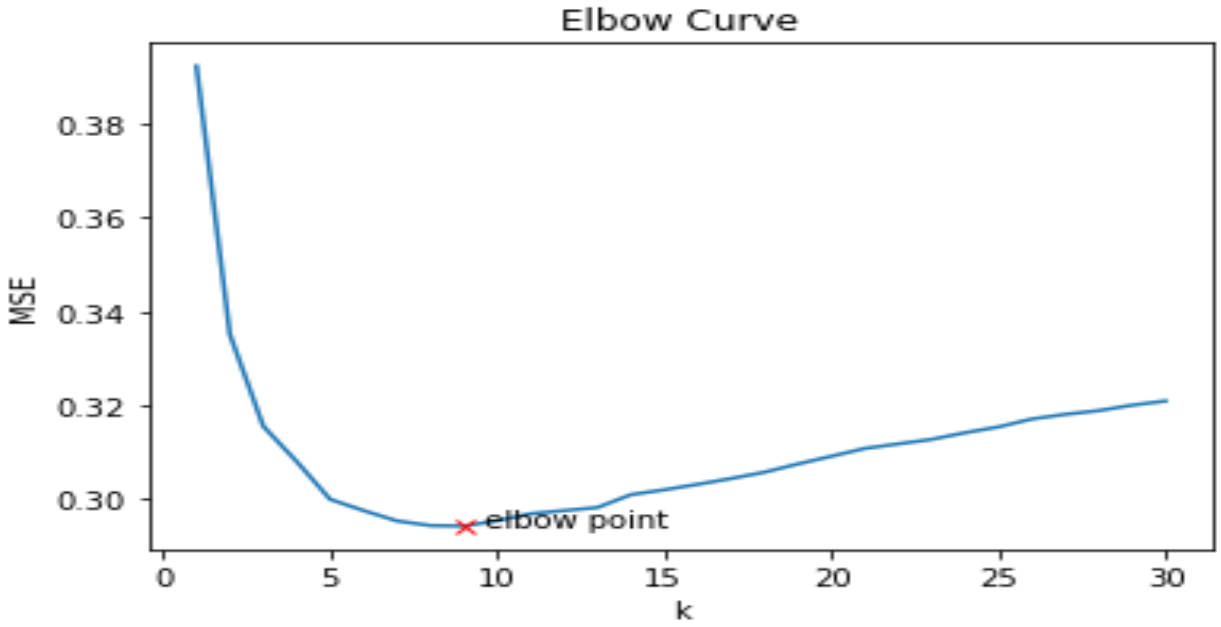


Fig. 3 Elbow curve for selecting the k value for KNN

3.3. Deep learning models

3.3.1 Feedforward neural network

The feedforward neural network (FNN) is one of two major forms of artificial neural networks (ANN), distinguished by the direction in which information flows between its layers. In ANN, initially, data enters the input layer, which subsequently transmits it to the hidden layers. In the initial phase, the interconnections between these layers assign random weights to each input. Each input neuron then introduces a bias. An activation function then evaluates the weighted sum, a combination of these weights and biases. The activation function plays a crucial role in determining which node should be activated for feature extraction. Eventually, the output is computed. This entire procedure is commonly referred to as forward propagation.

The feedforward neural network is a fundamental type of artificial neural network (ANN). In this ANN, data or input information follows a one-way path. It starts by entering the network through the input layer, then progresses to the output layer. While hidden layers can be incorporated between the input and output layers, they are not obligatory. A feedforward neural network typically uses forward propagation as the primary mode of information flow, and does not typically use backpropagation as the primary training method. An artificial neural network processes input data by calculating the weighted sum of the inputs, which includes a bias term. This computation is represented by the use of a transfer function as follows:

$$\sum_{i=1}^{n} wi * xi + b \tag{7}$$

The artificial neural network computes a weighted sum (Fig. 4), which is then fed into an activation function, which produces the output. Activation functions play an important part in determining whether a node should become active or not. Only activated nodes continue to the output layer. Several forms of activation functions are accessible; in this work, the ReLU (ectified Linear Unit) activation function is chosen.

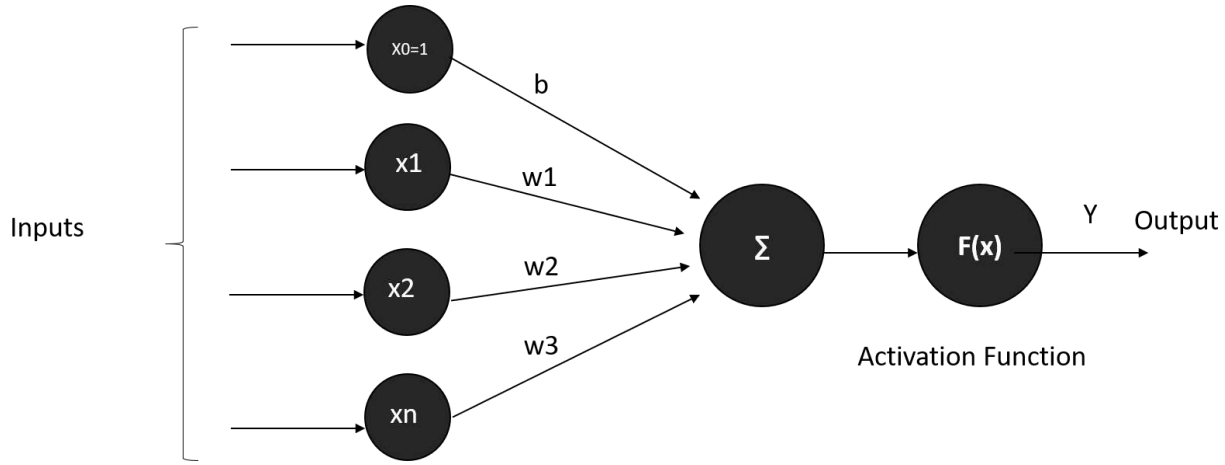


Fig. 4 Architecture of the Feedforard neural network along with activation function

3.3.2 Long Short-Term Memory (LSTM)

The LSTM is a recurrent neural network (RNN) architecture designed to address the challenges of collecting long-term dependencies in sequential data. Unlike conventional RNNs, LSTMs integrate specialized memory cells capable of retaining information over prolonged periods, thus mitigating the vanishing gradient issue (Fig. 5). These memory cells feature gating mechanisms that regulate information flow, empowering them to discern which data to retain or discard. Consequently, LSTMs work well in tasks necessitating the comprehension of extensive

dependencies, such as language modeling, speech recognition, and time series prediction. It comprises memory cells with gated units—input, forget, and output gates. In LSTM, the input gate controls new information entering the cell state, the forget gate removes outdated data, and the output gate selects important information for the next step. These gates help the model manage memory effectively, deciding what to keep or discard, which ensures smooth processing of sequences. The LSTM architecture effectively manages the retention and forgetting of information over successive time steps, ensuring nuanced processing of sequential data.

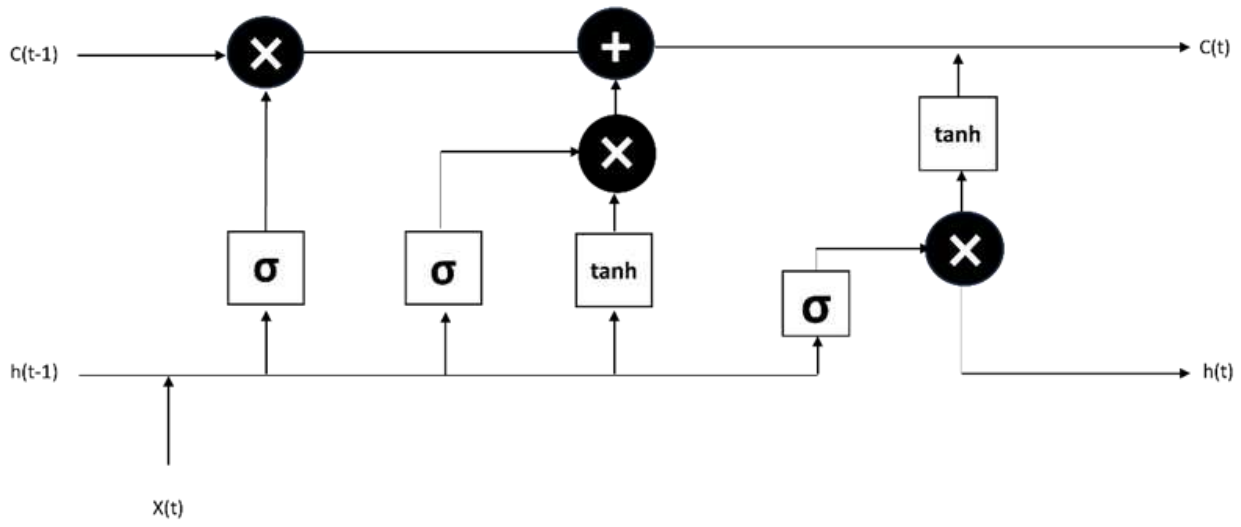


Fig. 5 Architecture of Long-Short Term Memory

3.4 Model evaluation

In this study, five statistical indices were used to evaluate the performance of machine learning and deep learning models for predicting the daily ET_o.

(i) Mean absolute error (MAE)

It is determined by averaging the absolute differences between the original (actual) and predicted values.

$$MAE = \frac{1}{N}\sum_{i=1}^{n} | ET_{est} - ET_{PM}| \quad (8)$$

(ii) Mean squared error (MSE)

It is similar to mean absolute error (MAE), but the important difference is how the average error is calculated. The MSE finds the average by squaring the discrepancies between the original and predicted values.

$$MSE = \frac{1}{N}\sum_{i=1}^{n}(ET_{est} - ET_{PM})^2 \quad (9)$$

(iii) Root mean square error (RMSE)

As implied by its name, RMSE is a straightforward calculation obtained by taking the square root of the mean square error.

$$RMSE = \sqrt{MSE} = \sqrt{\frac{1}{N}\sum_{i=1}^{n}(ET_{est} - ET_{PM})^2} \quad (10)$$

(iv) R-square (R^2)

The R^2 functions as a performance metric for the model, offering an assessment of its efficacy that remains independent of an absolute loss or gain. This metric is context-independent, making it valuable for comparing models when other metrics might fall short. As a result, it is often referred to as the R^2 as the coefficient of determination, which distinguishes it from other evaluation measures by serving as a baseline for model comparison.

$$R^2 = 1 - \frac{\sum_{i=1}^{n}(ET_{est} - ET_{PM})^2}{\sum_{i=1}^{n}(ET_{est} - ET_{mean})^2} \quad (11)$$

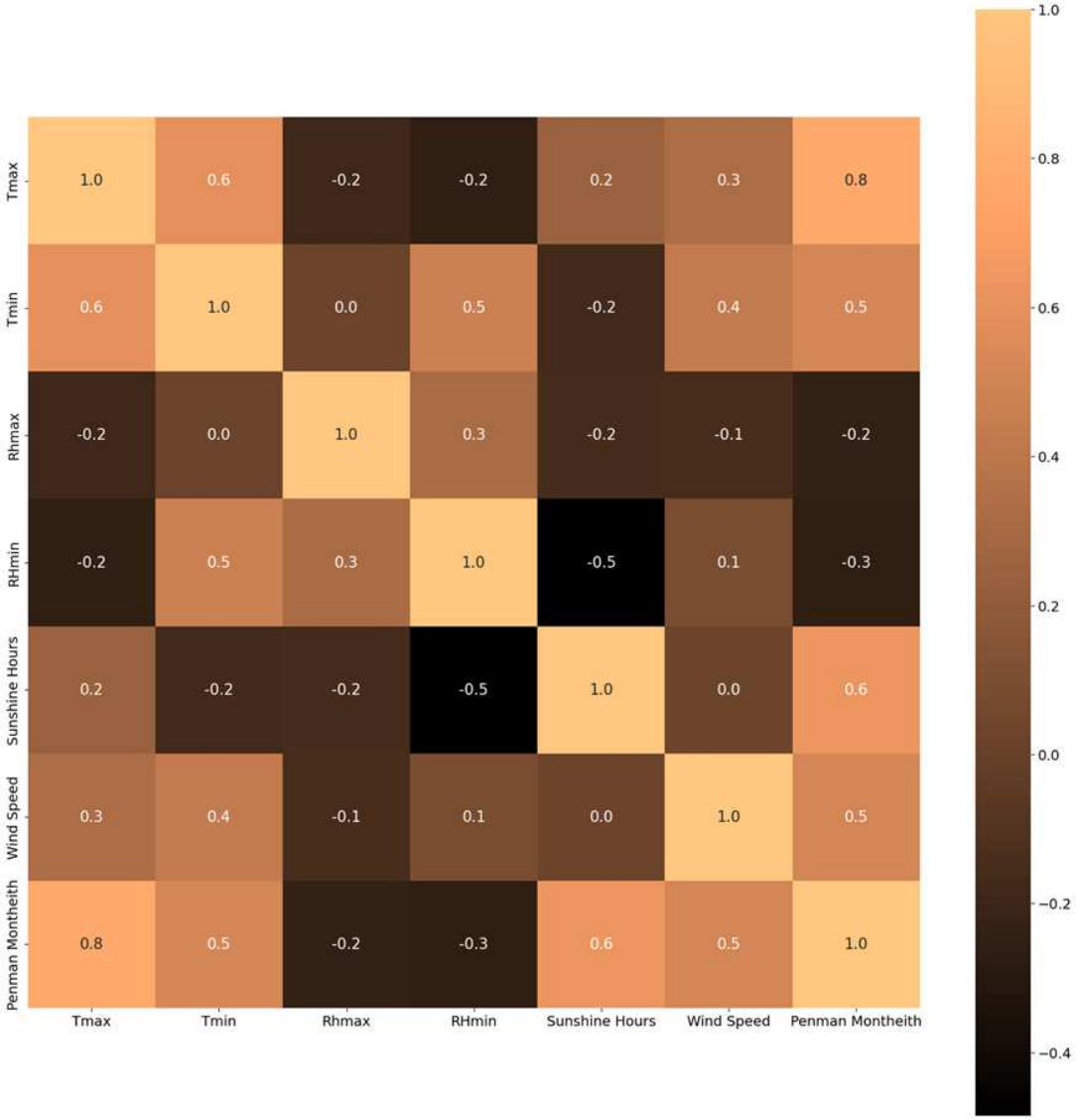
Where, ET_{est} is the estimated ET_o (mm/day); ET_{PM} is the PM-ET_o (mm/day); ET_{mean} is the average ET_o in mm/day; n is the number of data records.

4. Results and discussion

4.1 Correlation between ET_o and meteorological data

Figure 6 shows the relationship between PM-ET_o and the six climatological variables as a heat matrix. Among the relationships, sunshine hour and Tmax showed a significant ($p<0.01$) and positive relationship with PM-ET_o with r values of 0.8 and 0.6, respectively. However, Rmax and Rmin showed a negative correlation ($p<0.01$) with r values of 0.2 and 0.3, respectively. The wind speed and Tmin are positively correlated ($p<0.01$), with r values of 0.5 for both parameters. In order to accurately estimate ET_o, the examination of this heat matrix is essential to

445 formulating scenarios for combinations of meteorological parameters. We have listed the four
446 scenarios for the current study below:
447
448 ***Case 1:*** all six parameters of Penman-Monteith as input,
449 ***Case 2:*** all other meteorological variables excluding sunshine hour,
450 ***Case 3:*** Integrating temperature and relative humidity,
451 ***Case 4:*** taking only temperature (Tmax and Tmin) as input variables.
452



453
454 **Fig. 6 Heat matrix for correlation between PM- ET_o and meteorological variables**
455
456
457
458

4.2 Performance evaluation of ML and DL models with various input combinations

Figure 7 shows box plots that graphically contrast the observed ETo values with the estimated values produced by various models over the study period using different combinations of meteorological input variables. Case 1 (with all input parameters) The medians exhibit a high degree of similarity across all models, suggesting that the majority of models accurately forecast the central tendency. Additionally, the PM-ETo model demonstrates a narrower interquartile range (IQR) of 2.5. However, XGBoost and ANN exhibit greater variability (shown by longer whiskers) and a higher frequency of outliers. In Case 2, when all parameters except sunshine hour are considered, comparable distributions are obtained, albeit with significantly greater variability compared to employing all parameters. The XGBoost and Artificial Neural Network (Feedforward Neural Network) models have a higher frequency of outliers, indicating that they may be more sensitive to this particular set of parameters. Case 3, which includes temperature and humidity as input variables, The medians remain similar among models, but, the whiskers are longer, indicating a greater degree of variability. Among all the machine learning models, SVR has a lower interquartile range (IQR) in all three scenarios. There is a significant increase in the variability of predictions when only Tmax and Tmin are used as inputs (instance 4). The length of whiskers is greater, and there is a higher number of outliers, especially for models such as LR and ANN (FFNN) with an interquartile range (IQR) of 4.2. This indicates that models with fewer parameters result in less accurate predictions with more variations.

Figure 8 depicts scatter plots that demonstrate the correlations between PM-ET_o and ET_o calculated by the ML/DL models (for different R^2 values) during the testing periods. The performance of model is evaluated using the four statistical measures (R^2, MAE, MSE and RMSE) over the study period under different combinations of the meteorological input variables. Table 2 displays the performance evaluation of two deep learning (DL) approaches, namely feedforward neural network (FNN) and Long Short-Term Memory (LSTM), as well as five machine learning (ML) methods, namely linear regression, random forest (RF), support vector regression (SVR), K-nearest neighbors (KNN), and XGBoost models for the Phulnakhara canal command area.

4.2.1 Calibration of the models

For all four cases, 80% of the daily data is fed into the model, allowing the model to learn from the dataset by adjusting its parameters to reduce the error between predicted and actual outcomes. This involves fine-tuning the model parameters to improve accuracy and performance with various performance metrics, and the results are as follows.

Case 1 (with all input parameters): The RF model showed outstanding performance (R^2 = 0.99, RMSE = 0.23, MSE = 0.053, and MAE = 0.169) compared to the other assessed models, namely XGB (R^2 = 0.988, MAE = 0.113, MSE = 0.023, RMSE = 0.153), ANN (FNN) (R^2 = 0.966, MAE = 0.197, MSE = 0.067, RMSE = 0.259), LSTM (R^2 = 0.960, MAE = 0.220, MSE = 0.078, RMSE = 0.280), KNN (R^2 = 0.964, MAE = 0.198, MSE = 0.071, RMSE = 0.267), and LR (R^2 = 0.915, MAE = 0.290, MSE = 0.171, RMSE = 0.413), respectively.

Case 2: The performance of ML/DL models for estimation of ET_o with the input parameters of temperature, wind speed, and RH is as follows: RF (R^2 = 0.98, RMSE = 0.183, MSE = 0.137, and MAE = 0.033) is followed by XGB (R^2 = 0.936, MAE = 0.264, MSE = 0.127, RMSE = 0.356), SVR (R^2 = 0.888, Adj R^2 = 0.888, MAE = 0.348, MSE = 0.225, RMSE = 0.474), ANN (FNN) (Calibration: R^2 = 0.879, MAE = 0.370, MSE = 0.241, RMSE = 0.491), RF (R^2 = 0.983, MAE = 0.137, MSE = 0.033, RMSE = 0.183), LR (R^2 = 0.817, MAE = 0.458, MSE = 0.368, RMSE = 0.606), LSTM (R^2 = 0.855, MAE = 0.412, MSE = 0.291, RMSE = 0.540), and KNN (R^2 = 0.785, MAE = 0.494, MSE = 0.430, RMSE = 0.656), respectively.

Case 3: Similarly, with the input parameters of maximum and minimum temperature and RH, the RF (R^2 = 0.97, RMSE = 0.247, MSE = 0.416, and MAE = 0.187) is followed by XGB (R^2 = 0.880, MAE = 0.374, MSE = 0.240, RMSE = 0.490), SVR (R^2 = 0.806, MAE = 0.469, MSE = 0.389, RMSE = 0.623), ANN (FNN) (R^2 = 0.792, MAE = 0.497, MSE = 0.417, RMSE = 0.646), LSTM (R^2 = 0.773, MAE = 0.518, MSE = 0.456, RMSE = 0.675), LR (R^2 = 0.760, MAE = 0.544, MSE = 0.482, RMSE = 0.694) and KNN (R^2 = 0.824, Adj R^2 = 0.824, MAE = 0.454, MSE = 0.352, RMSE = 0.594) respectively.

Case 4: With input parameters as temperature (Tmax and Tmin), the performance of the models were RF (R^2 = 0.88, RMSE = 0.488, MSE = 0.238, and MAE = 0.351) followed by the XGB (R^2 = 0.812, MAE = 0.461, MSE = 0.375, RMSE = 0.613), SVR (R^2 = 0.757, MAE = 0.523, MSE = 0.486, RMSE = 0.697), KNN (R^2 = 0.738, MAE = 0.559, MSE = 0.540, RMSE = 0.734). LSTM (R^2 = 0.732, MAE =0.564, MSE =0.538, RMSE =0.734), ANN (FNN) (R^2 = 0.728, MAE = 0.553, MSE = 0.544, RMSE = 0.737) and LR (R^2 = 0.699, MAE = 0.603, MSE = 0.604, RMSE = 0.777), respectively. Sammen et al. (2023) reported similar results, confirming the significant reduction in RF performance during validation.

4.2.2 Testing/validation of the model

After training, the model is tested against the remaining 20% of the data to evaluate its performance to ensure the model generalizes well to unseen data and the results are as below.

Case 1: Table 2 clearly shows that all but one of the machine learning (ML) and deep learning (DL) models performed exceptionally well, with an R^2 value greater than 0.96. The only model that did not do this well was linear regression with all of the input data. The SVM model had outstanding performance (R^2 = 0.98, RMSE = 0.23, MSE = 0.053, and MAE = 0.169) compared to XGB (R^2 = 0.974, MAE = 0.169, MSE = 0.053, RMSE = 0.230), RF (R^2 = 0.970, MAE = 0.170, MSE = 0.060, RMSE = 0.245), ANN(FNN) (R^2 = 0.968, MAE = 0.198, MSE = 0.065, RMSE = 0.255), LSTM (R^2 = 0.960, MAE = 0.223, MSE = 0.082, RMSE = 0.286), KNN (R^2 = 0.957, MAE = 0.218, MSE = 0.086, RMSE = 0.294), and LR (R^2 = 0.930, MAE = 0.292, MSE = 0.142, RMSE = 0.377) when all parameters were used as input.

Case 2: The performance of models for the input parameters of temperature, wind speed, and RH is as follows: SVM (R^2 = 0.88, RMSE =0.495, MSE = 0.245, and MAE = 0.359) is followed by ANN (FNN) (R^2 = 0.881, MAE = 0.377, MSE = 0.245, RMSE = 0.495), XGB (R^2 = 0.876, Adj R^2 = 0.876, MAE = 0.376, MSE = 0.254, RMSE = 0.504), RF (R^2 = 0.873, MAE = 0.378, MSE = 0.260, RMSE = 0.510), LSTM (R^2 = 0.856, MAE = 0.414, MSE = 0.296, RMSE = 0.544), LR (R^2 = 0.836, MAE = 0.457, MSE = 0.337, RMSE = 0.580), and KNN (R^2 = 0.738, MAE = 0.559, MSE = 0.540, RMSE = 0.734).

Case 3: Similarly, with input parameters of maximum and minimum temperature and RH, the SVR model (R^2 =0 .80, RMSE = 0.645, MSE = 0.416, and MAE = 0.484) is followed by ANN (FNN) (R^2 = 0.792, Adj R^2 = 0.792, MAE = 0.504, MSE = 0.428, RMSE = 0.654), XGB (R^2 = 0.782, Adj R^2 = 0.782, MAE = 0.502, MSE = 0.446, RMSE = 0.668), RF (R^2 = 0.782, Adj R^2 = 0.782, MAE = 0.505, MSE = 0.447, RMSE = 0.669), LSTM (R^2 = 0.773, Adj R^2 = 0.773, MAE = 0.518, MSE = 0.456, RMSE = 0.675), LR (R^2 = 0.760, Adj R^2 = 0.760, MAE = 0.550, MSE = 0.492, RMSE = 0.701) and RF (R^2 = 0.782, Adj R^2 = 0.782, MAE = 0.505, MSE = 0.447, RMSE = 0.669).

Case 4: The only taking temperature (Tmax and Tmin) as input parameter, the performance of the models were KNN (R^2 = 0.79, RMSE = 0.656, MSE = 0.43, and MAE = 0.494) followed by SVR (R^2 = 0.761, MAE = 0.532, MSE = 0.492, RMSE = 0.701), XGB (R^2 = 0.745, MAE = 0.552, MSE = 0.526, RMSE = 0.725), ANN (FNN) (R^2 = 0.73, RMSE = 0.55, MSE = 0.55, and MAE =0.74), LSTM (R^2 = 0.723, RMSE = 0.572, MSE = 0.568, and MAE =0.754), LR (R^2 = 0.695, MAE = 0.613, MSE = 0.630, RMSE = 0.793), and RF (R^2 = 0.690, MAE = 0.606, MSE = 0.639, RMSE = 0.799).

Figure 9 depicts the Taylor diagram for both PM-ETo and ML/DL-predicted ETo. It shows the relationship between correlation coefficient (r), the standard deviation (SD). the root mean square deviation (RMSD). The best model is typically the one that is closest to the reference point, indicating high correlation, appropriate standard deviation, and low RMSE. The closer the

point is to the horizontal axis, the higher the correlation. The closer the radial distance to the observation point, the closer the standard deviation of the model is to that of the observations. A smaller RMSE (closer to the reference point) indicates a better fit. It is evident that among the DL models, LSTM models, and ML models, SVR exhibits excellent performance, having the greatest correlation coefficient with the lowest standard deviation and RMSD for all parameters.

Table 2: Performance of ML and DL models for calibration and validation with evaluation parameters

Parameters	Model	Calibration				Validation			
		R^2	MAE	MSE	RMSE	R^2	MAE	MSE	RMSE
All parameters	Linear Regression	0.915	0.290	0.171	0.413	0.930	0.292	0.142	0.377
	Random Forest	0.996	0.062	0.007	0.085	0.970	0.170	0.060	0.245
	XG Boost	0.988	0.113	0.023	0.153	0.974	0.169	0.053	0.230
	SVR	0.980	0.140	0.039	0.198	0.977	0.145	0.047	0.216
	KNN Regression	0.964	0.198	0.071	0.267	0.957	0.218	0.086	0.294
	ANN(FNN)	0.966	0.197	0.067	0.259	0.968	0.198	0.065	0.255
	LSTM	0.960	0.220	0.078	0.280	0.960	0.223	0.082	0.286
Temperature, Windspeed, and Relative Humidity	Linear Regression	0.817	0.458	0.368	0.606	0.836	0.457	0.337	0.580
	Random Forest	0.983	0.137	0.033	0.183	0.873	0.378	0.260	0.510
	XG Boost	0.936	0.264	0.127	0.356	0.876	0.376	0.254	0.504
	SVR	0.888	0.348	0.225	0.474	0.888	0.359	0.245	0.495
	KNN Regression	0.785	0.494	0.430	0.656	0.738	0.559	0.540	0.734
	ANN(FNN)	0.879	0.370	0.241	0.491	0.881	0.377	0.245	0.495
	LSTM	0.855	0.412	0.291	0.540	0.856	0.414	0.296	0.544
Temperature and Relative Humidity	Linear Regression	0.760	0.544	0.482	0.694	0.760	0.550	0.492	0.701
	Random Forest	0.969	0.187	0.061	0.247	0.782	0.505	0.447	0.669
	XG Boost	0.880	0.374	0.240	0.490	0.782	0.502	0.446	0.668
	SVR	0.806	0.469	0.389	0.623	0.797	0.484	0.416	0.645

	KNN Regression	0.824	0.454	0.352	0.594	0.781	0.508	0.449	0.670
	ANN(FNN)	0.792	0.497	0.417	0.646	0.792	0.504	0.428	0.654
	LSTM	0.773	0.518	0.456	0.675	0.765	0.529	0.481	0.694
Maximum Temperature, Minimum Temperature	Linear Regression	0.699	0.603	0.604	0.777	0.695	0.613	0.630	0.793
	Random Forest	0.881	0.351	0.238	0.488	0.690	0.606	0.639	0.799
	XG Boost	0.812	0.461	0.375	0.613	0.745	0.552	0.526	0.725
	SVR	0.757	0.523	0.486	0.697	0.761	0.532	0.492	0.701
	KNN Regression	0.738	0.559	0.540	0.734	0.785	0.494	0.430	0.656
	ANN(FNN)	0.728	0.553	0.544	0.737	0.733	0.550	0.551	0.742
	LSTM	0.732	0.564	0.538	0.734	0.723	0.572	0.568	0.754

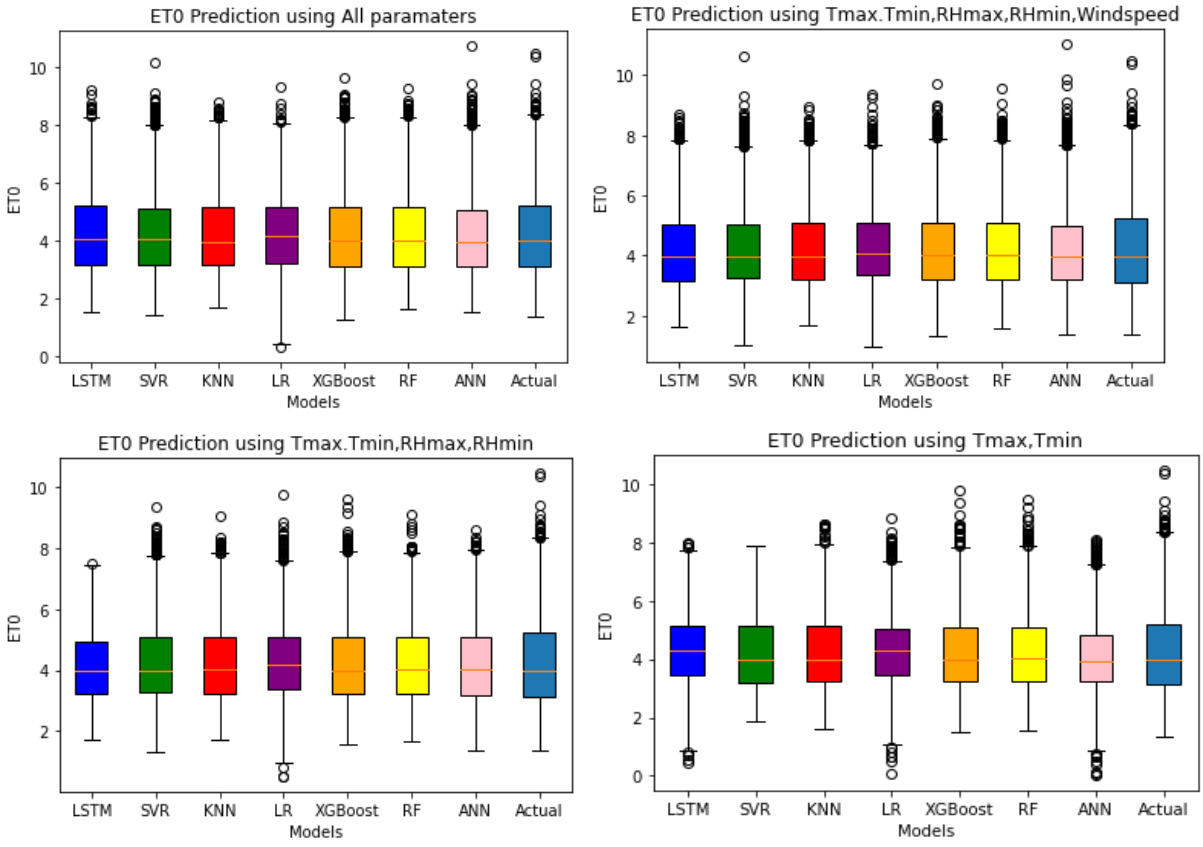
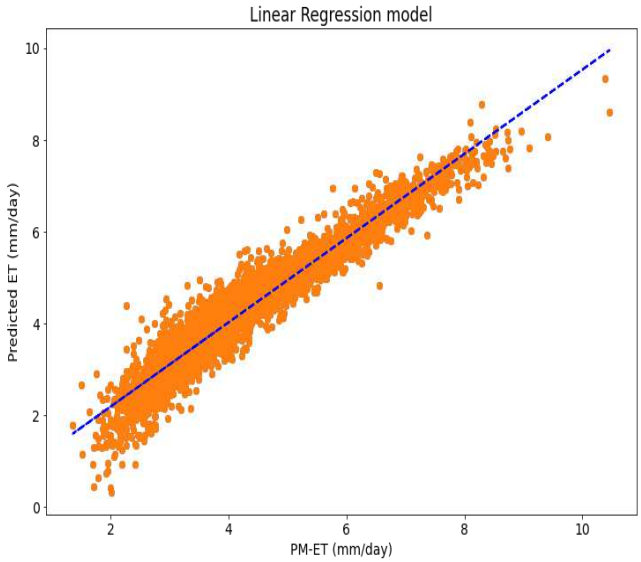
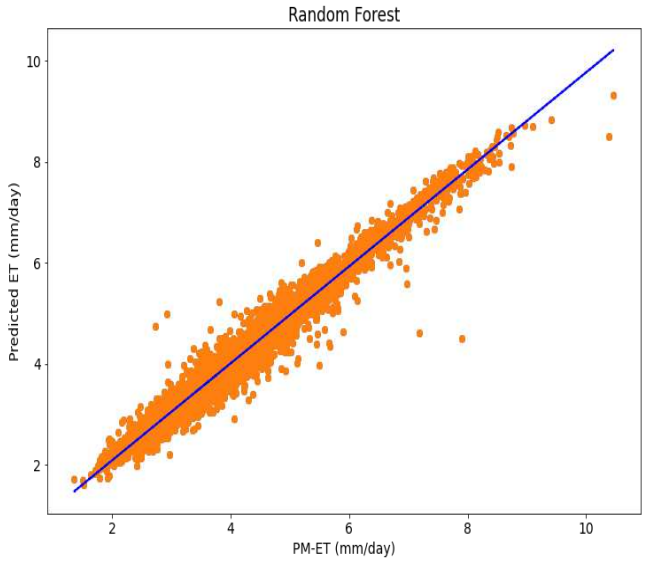
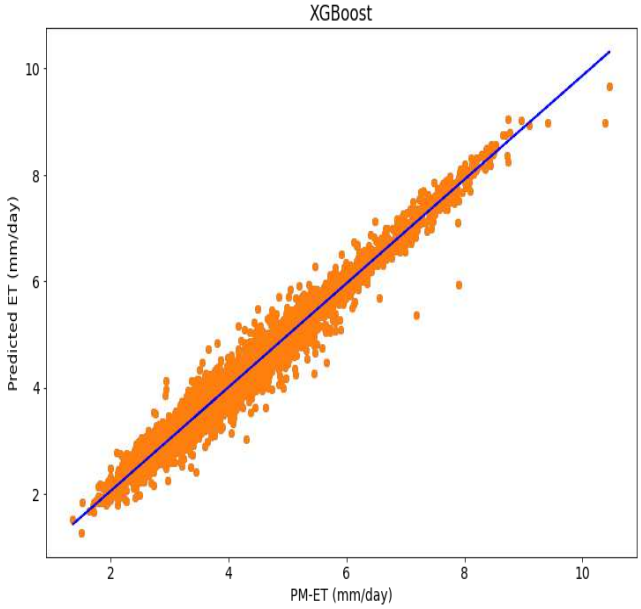


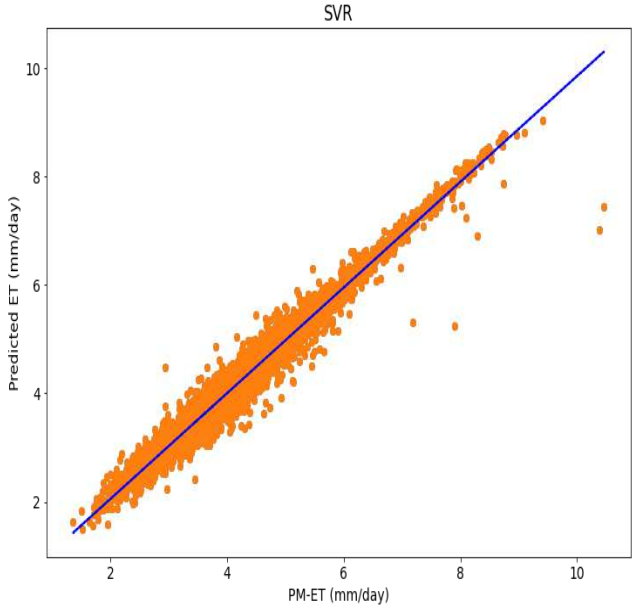
Figure 7. Comparison of observed and estimated ET_o by different models (liner regression , random forest, XGBoost, SVR and KNN regression) with variable input parameters during the validation period at the Phulnakhara canal command area

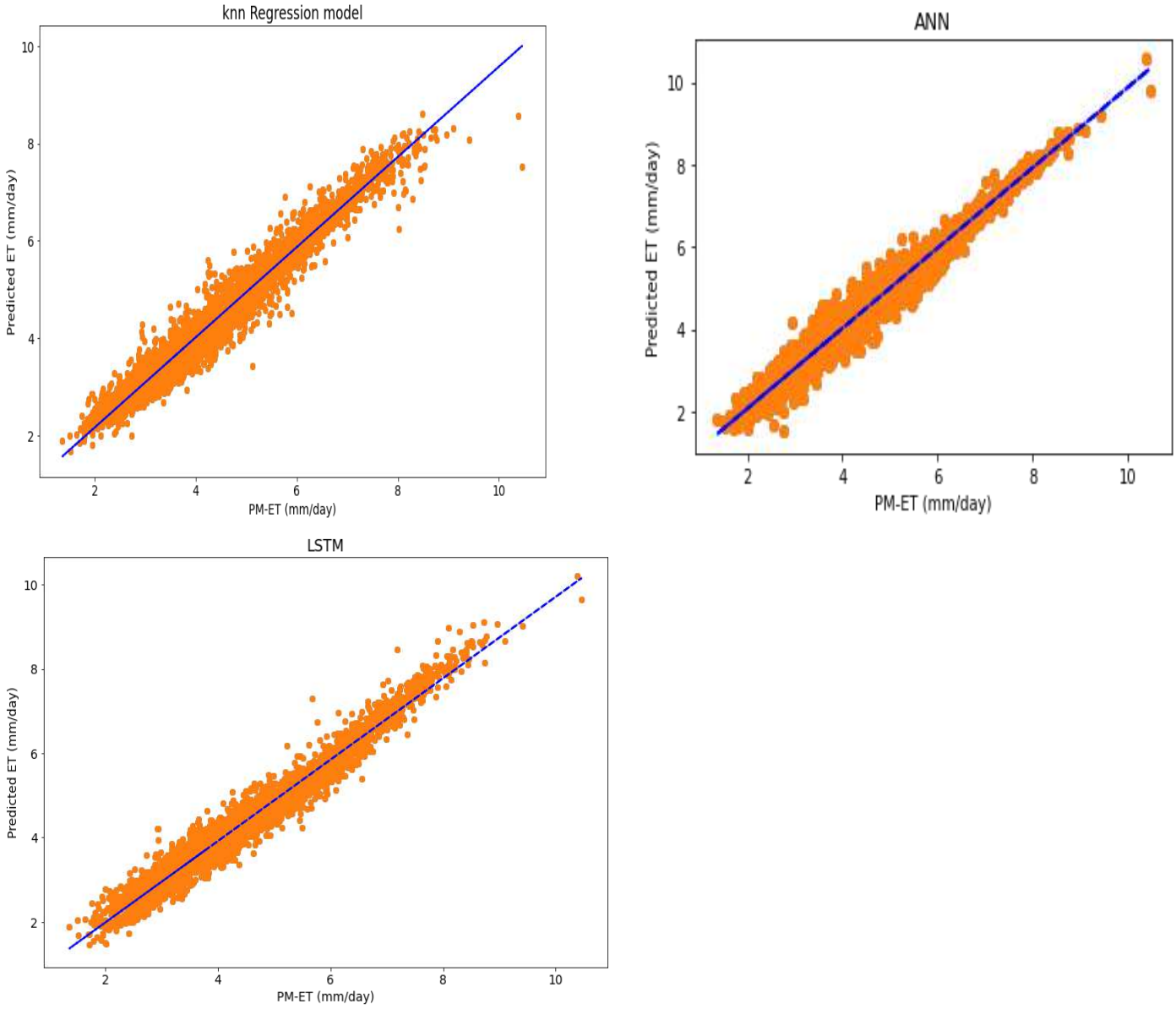
591


Linear Regression model
Predicted ET (mm/day)
PM-ET (mm/day)
0
2
4
6
8
10


Random Forest
Predicted ET (mm/day)
PM-ET (mm/day)
2
4
6
8
10


XGBoost
Predicted ET (mm/day)
PM-ET (mm/day)
2
4
6
8
10


SVR
Predicted ET (mm/day)
PM-ET (mm/day)
2
4
6
8
10



592

593 Figure 8. Scatter plots of the ET referred as ET_o and those calculated by the five ML models (a)
594 linear regression, (b) random forest, (c) XGBoost, (d) SVR, (e) KNN regression and two DL
595 models (f) Feedforward neural network (FNN), and (g) LSTM with all input variables during the
596 testing period at the Phulnakhara canal command area

597

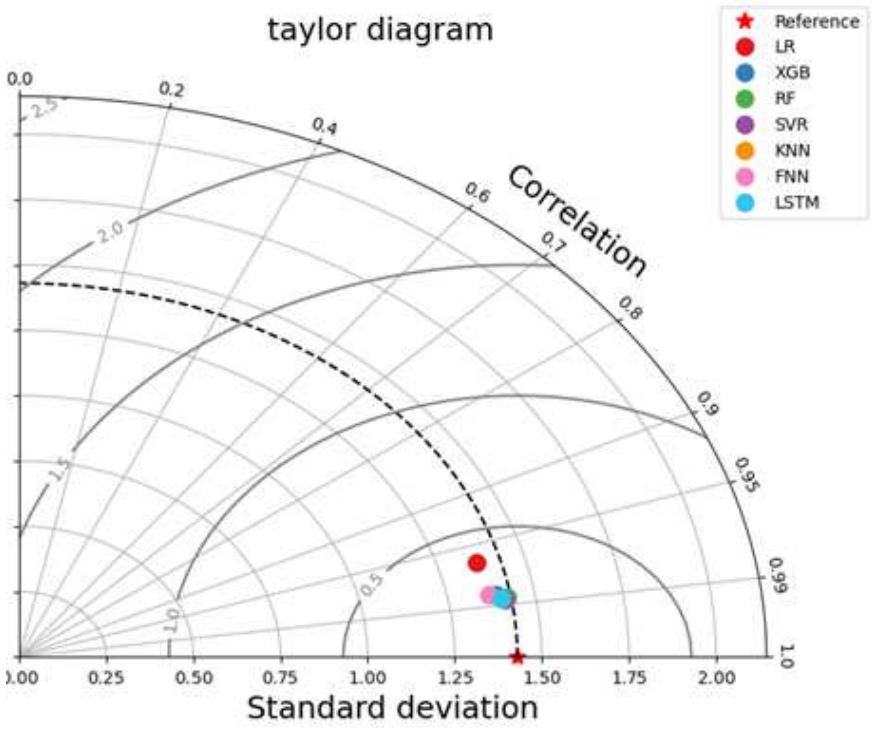


Fig. 9 Taylors diagram for ML and DL models

5. Conclusions

An accurate assessment of evapotranspiration is essential many studies such as crop yield prediction, irrigation scheduling and hydrological modeling. In data scarce regions, the machine learning and deep learning models has proven to be a powerful tool for accurately predicting the evapotranspiration. Therefore, in this study, five machine learning (ML) and two deep learning (DL) models were used to estimate the ET_o over the Phulnahara canal command area using various combinations of meteorological parameters. ML/DL-based models predicted a strong convergence between the PM-ET_o and the ET_o. The RHmax and RHmin have a negative correlation with a correlation coefficient (r) of -0.2 and -0.3, respectively, while the sunshine hour and Tmax have a strong positive correlation with r of 0.8 and 0.6, respectively. when all the parameters except sunshine hours (case 2) was considered for evaluation of ETo, had lower model evaluation indices than including all the six parameters required to estimate ET_o (case 1). This emphasizes the critical role of sunlight hours in estimating the ET_o. The inclusion of the sunshine hour parameter significantly improved machine learning models' performance. Furthermore, the absence of sunshine hour coupled with windspeed (case 3) resulted in a further decrease in the model evaluation indices. In all three cases, the support vector regression (SVR) model emerged as the most robust model for estimating ET_o. Lastly, we only considered Tmax and Tmin for ET_o estimation, with KNN being the best performing model. Among the DL

models, the LSTM performed better compared to the ANN (FNN) model in all cases. The median values across different models are relatively close to each other and to the PM-ET_o in all cases. This indicates that most models are reasonably good at predicting the central tendency of ET0. The IQR tends to be narrowest when using all parameters and increases as fewer parameters are used. Models generally show more outliers and longer whiskers when fewer input parameters are used. This indicates higher variability and less robust predictions with fewer inputs. This suggests that more input parameters lead to more consistent predictions. In conclusion, our study gives useful information about the complicated processes involved in estimating ET_o. It emphasizes the significance of certain metrological parameters and the usefulness of various modeling methods based on data availability. These findings provide practical direction for academics and practitioners working in areas with various data restrictions, allowing for more precise and reliable ET_o forecasts.

Acknowledgements

The author thanks the ICAR-Indian Institute of Water Management, Bhubaneswar, Odisha, India, for providing the required facilities to perform this research.

Conflict of interest

The authors have declared no conflicts of interest.

Funding

No funding has been received from any source.

Data availability

The data are available on request from the corresponding author.

Authors contribution

Ajit Kumar Nayak: Code writing, data analysis and original draft writing

A Sarangi: Editing the manuscript and supervision

S Pradhan: Estimating the ET_o by Penman Monteith method

R K Panda: Data screening and critical review

N M Jeepsa: Debugging the code

Mithlesh Kumar: LSTM data analysis

B S Satpathy: Collection of literatures and review of literature

References

Aly, M. S., Darwish, S. M., & Aly, A. A. (2024). High performance machine learning approach for reference evapotranspiration estimation. Stochastic Environmental Research and Risk Assessment, 38(2), 689-713. https://doi.org/10.1007/s00477-023-02594-y

Amani, S., & Shafizadeh-Moghadam, H. (2023). A review of machine learning models and influential factors for estimating evapotranspiration using remote sensing and ground-based data.Agricultural Water Management, 284, 108324. https://doi.org/10.1016/j.agwat.2023.108324

Ayaz, A., Rajesh, M., Singh, S. K., & Rehana, S. (2021). Estimation of reference evapotranspiration using machine learning models with limited data. AIMS Geosci, 7(3), 268-290. https://doi.org/10.3934/geosci.2021016

Bayram, S., & Çıtakoğlu, H. (2023). Modelling monthly reference evapotranspiration process in Turkey: application of machine learning methods. Environmental Monitoring and Assessment, 195(1), https://doi.org/10.1007/s10661-022-10662-z

Bellido-Jiménez, J. A., Estévez, J., & García-Marín, A. P. (2021). New machine learning approaches to improve reference evapotranspiration estimates using intra-daily temperature-based variables in a semi-arid region of Spain. Agricultural Water Management, 245. https://doi.org/10.1016/j.agwat.2020.106558

Biau, G. (2012). Analysis of a random forests model. The Journal of Machine Learning Research, 13(1), 1063-1095.

Biau, G., & Scornet, E. (2016). A random forest guided tour. Test, 25(2). https://doi.org/10.1007/s11749-016-0481-7

Bijlwan, A., Pokhriyal, S., RANJAN, R., Singh, R. K., & Jha, A. (2024). Machine learning methods for estimating reference evapotranspiration. Journal of Agrometeorology, 26(1), 63-68. https://doi.org/10.54386/jam.v26i1.2462

Boswell, D. (2002). Introduction to support vector machines. Departement of Computer Science and Engineering University of California San Diego, 11, 16-17.

Breiman, L. (2001). Random forests. Machine Learning, 45(1). https://doi.org/10.1023/A:1010933404324

Chandrahas, S. N., Choudhary, B. S., Vishnu Teja, M., Venkataramayya, M. S., & Krishna Prasad, N. S. R. (2022). XG Boost Algorithm to Simultaneous Prediction of Rock Fragmentation and Induced Ground Vibration Using Unique Blast Data. Applied Sciences (Switzerland), 12(10). https://doi.org/10.3390/app12105269

Chia, M. Y., Huang, Y. F., Koo, C. H., & Fung, K. F. (2020). Recent advances in evapotranspiration estimation using artificial intelligence approaches with a focus on hybridization techniques—A review. In Agronomy, 10 (1). https://doi.org/10.3390/agronomy10010102

Chia, M. Y., Huang, Y. F., Koo, C. H., Ng, J. L., Ahmed, A. N., & El-Shafie, A. (2022). Long-term forecasting of monthly mean reference evapotranspiration using deep neural network: A comparison of training strategies and approaches. Applied Soft Computing, 126, 109221. https://doi.org/10.1016/j.asoc.2022.109221

da Silva Júnior, J. C., Medeiros, V., Garrozi, C., Montenegro, A., & Gonçalves, G. E. (2019). Random forest techniques for spatial interpolation of evapotranspiration data from Brazilian's Northeast. Computers and Electronics in Agriculture, 166. https://doi.org/10.1016/j.compag.2019.105017

Dimitriadou, S., & Nikolakopoulos, K. G. (2022). Multiple Linear Regression Models with Limited Data for the Prediction of Reference Evapotranspiration of the Peloponnese, Greece. Hydrology, 9(7). https://doi.org/10.3390/hydrology9070124

Fan, J., Yue, W., Wu, L., Zhang, F., Cai, H., Wang, X., Lu, X., & Xiang, Y. (2018). Evaluation of SVM, ELM and four tree-based ensemble models for predicting daily reference evapotranspiration using limited meteorological data in different climates of China. Agricultural and Forest Meteorology, 263, 225–241. https://doi.org/10.1016/j.agrformet.2018.08.019

Gocić, M., Motamedi, S., Shamshirband, S., Petković, D., Ch, S., Hashim, R., & Arif, M. (2015). Soft computing approaches for forecasting reference evapotranspiration. Computers and Electronics in Agriculture, 113. https://doi.org/10.1016/j.compag.2015.02.010

Granata, F. (2019). Evapotranspiration evaluation models based on machine learning algorithms—A comparative study. Agricultural Water Management, 217. https://doi.org/10.1016/j.agwat.2019.03.015

Hao, P., Di, L., & Guo, L. (2022). Estimation of crop evapotranspiration from MODIS data by combining random forest and trapezoidal models. Agricultural Water Management, 259. https://doi.org/10.1016/j.agwat.2021.107249

Huang, G., Wu, L., Ma, X., Zhang, W., Fan, J., Yu, X., Zeng, W., & Zhou, H. (2019). Evaluation of CatBoost method for prediction of reference evapotranspiration in humid regions. Journal of Hydrology, 574. https://doi.org/10.1016/j.jhydrol.2019.04.085

Huang, S. (2022). Linear regression analysis. In International Encyclopedia of Education: Fourth Edition. https://doi.org/10.1016/B978-0-12-818630-5.10067-3

Irmak, S., Irmak, A., Allen, R. G., & Jones, J. W. (2003). Solar and Net Radiation-Based Equations to Estimate Reference Evapotranspiration in Humid Climates. Journal of Irrigation and Drainage Engineering, 129(5). https://doi.org/10.1061/(asce)0733-9437(2003)129:5(336)

Kumar, M., Raghuwanshi, N. S., Singh, R., Wallender, W. W., & Pruitt, W. O. (2002). Estimating Evapotranspiration using Artificial Neural Network. Journal of Irrigation and Drainage Engineering, 128(4). https://doi.org/10.1061/(asce)0733-9437(2002)128:4(224)

Mallikarjuna, P., Jyothy, S. A., & Sekhar Reddy, K. C. (2012). Daily Reference Evapotranspiration Estimation using Linear Regression and ANN Models. Journal of The Institution of Engineers (India): Series A, 93(4). https://doi.org/10.1007/s40030-013-0030-2

Maulud, D., & Abdulazeez, A. M. (2020). A Review on Linear Regression Comprehensive in Machine Learning. Journal of Applied Science and Technology Trends, 1(4). https://doi.org/10.38094/jastt1457

Mo, H., Sun, H., Liu, J., & Wei, S. (2019). Developing window behavior models for residential buildings using XGBoost algorithm. Energy and Buildings, 205. https://doi.org/10.1016/j.enbuild.2019.109564

Raza, A., Shoaib, M., Faiz, M. A., Baig, F., Khan, M. M., Ullah, M. K., & Zubair, M. (2020). Comparative Assessment of Reference Evapotranspiration Estimation Using Conventional Method and Machine Learning Algorithms in Four Climatic Regions. Pure and Applied Geophysics, 177(9). https://doi.org/10.1007/s00024-020-02473-5

Rana, G., & Katerji, N. (2000). Measurement and estimation of actual evapotranspiration in the field under Mediterranean climate: A review. European Journal of Agronomy, 13(2–3). https://doi.org/10.1016/S1161-0301(00)00070-8

Sammen, S. S., Kisi, O., Al-Janabi, A. M. S., & Elbeltagi, A. (2023). Predicting reference evapotranspiration in semi-arid-region by regression-based machine learning methods using limited climatic inputs. https://doi.org/10.21203/rs.3.rs-2600302/v1

Sattari, M. T., Apaydin, H., Band, S. S., Mosavi, A., & Prasad, R. (2021). Comparative analysis of kernel-based versus ANN and deep learning methods in monthly reference evapotranspiration estimation. Hydrology and Earth System Sciences, 25(2), 603–618. https://doi.org/10.5194/hess-25-603-2021

Schmidt, A. F., & Finan, C. (2018). Linear regression and the normality assumption. In Journal of Clinical Epidemiology (Vol. 98). https://doi.org/10.1016/j.jclinepi.2017.12.006

Shiri, J., Nazemi, A. H., Sadraddini, A. A., Landeras, G., Kisi, O., Fakheri Fard, A., & Marti, P. (2014). Comparison of heuristic and empirical approaches for estimating reference evapotranspiration from limited inputs in Iran. Computers and Electronics in Agriculture, 108, 230–241. https://doi.org/10.1016/j.compag.2014.08.007

Song, X., Lu, F., Xiao, W., Zhu, K., Zhou, Y., & Xie, Z. (2019). Performance of 12 reference evapotranspiration estimation methods compared with the Penman–Monteith method and

the potential influences in northeast China. Meteorological Applications, 26(1). https://doi.org/10.1002/met.1739

Tikhamarine, Y., Malik, A., Kumar, A., Souag-Gamane, D., & Kisi, O. (2019). Estimation of monthly reference evapotranspiration using novel hybrid machine learning approaches. Hydrological sciences journal, 64(15), 1824-1842. https://doi.org/10.1080/02626667.2019.1678750

Treder, W., Klamkowski, K., Wójcik, K., & Tryngiel-Gać, A. (2023). Evapotranspiration Estimation Using Machine Learning Methods. Journal of Horticultural Research. https://doi.org/10.2478/johr-2023-0033

Wang, S., Lian, J., Peng, Y., Hu, B., & Chen, H. (2019). Generalized reference evapotranspiration models with limited climatic data based on random forest and gene expression programming in Guangxi, China. Agricultural Water Management, 221. https://doi.org/10.1016/j.agwat.2019.03.027

Wu, L., Peng, Y., Fan, J., & Wang, Y. (2019). Machine learning models for the estimation of monthly mean daily reference evapotranspiration based on cross-station and synthetic data. Hydrology Research, 50(6), 1730-1750. https://doi.org/10.2166/nh.2019.060

Wu, T., Zhang, W., Jiao, X., Guo, W., & Alhaj Hamoud, Y. (2021). Evaluation of stacking and blending ensemble learning methods for estimating daily reference evapotranspiration. Computers and Electronics in Agriculture, 184. https://doi.org/10.1016/j.compag.2021.106039

Yamaç, S. S. (2021). Artificial intelligence methods reliably predict crop evapotranspiration with different combinations of meteorological data for sugar beet in a semiarid area. Agricultural Water Management, 254. https://doi.org/10.1016/j.agwat.2021.106968

Yamaç, S. S., & Todorovic, M. (2020). Estimation of daily potato crop evapotranspiration using three different machine learning algorithms and four scenarios of available meteorological data. Agricultural Water Management, 228. https://doi.org/10.1016/j.agwat.2019.105875

Yin, L., Tao, F., Chen, Y., Liu, F., & Hu, J. (2021). Improving terrestrial evapotranspiration estimation across China during 2000–2018 with machine learning methods. Journal of Hydrology, 600. https://doi.org/10.1016/j.jhydrol.2021.126538

Yong, S. L. S., Ng, J. L., Huang, Y. F., & Ang, C. K. (2023). Estimation of reference crop evapotranspiration with three different machine learning models and limited meteorological variables. Agronomy, 13(4), 1048. https://doi.org/10.3390/agronomy13041048